Chem. Senses 39: 91–105, 2014
doi:10.1093/chemse/bjt057
Advance Access publication November 11, 2013

A Comparison Between the Human Sense of Smell and Neural Activity in the Olfactory Bulb of Rats

Zu Soh[1], Maki Saito[2], Yuichi Kurita[1], Noboru Takiguchi[3], Hisao Ohtake[4] and Toshio Tsuji[1]

[1]Department of System Cybernetics, Institute of Engineering, Hiroshima University, 1-4-1 Kagamiyama, Higashi-Hiroshima, Hiroshima 739–8527, Japan, [2]Department of System Cybernetics, Graduate School of Engineering, Hiroshima University, 1-4-1 Kagamiyama, Higashi-Hiroshima, Hiroshima 739–8527, Japan, [3]Division of Material Sciences, Graduate School of Natural Science and Technology, Kanazawa University, Kakuma, Kanazawa 920–1192, Japan and [4]Department of Biotechnology, Graduate School of Engineering, Osaka University, 2-1 Yamadaoka, Suita Osaka 565–0871, Japan

Correspondence to be sent to: Zu Soh, Department of System Cybernetics, Institute of Engineering, Hiroshima University, 1-4-1 Kagamiyama, Higashi-Hiroshima, Hiroshima 739–8527, Japan. e-mail: *sozu@bsys.hiroshima-u.ac.jp*

Accepted September 4, 2013

Abstract

Generally, odor qualities are evaluated via sensory tests in which predefined criteria are assessed by panelists and stochastically analyzed to reduce human inconsistencies. Because this method requires multiple, well-trained human subjects, a more convenient approach is required to enable predictions of odor qualities. In this article, we propose an approach involving linking internal states of the olfactory system with perceptual characteristics. In the study, the glomerular responses of rats were taken to represent internal olfactory system states. Similarities between the glomerular responses of rats were quantified by correlations between glomerular activity patterns, overlap rate of strongly activated part across glomerular activity patterns, and the similarity between histograms of the strength of activity. These indices were then compared with perceptual similarities measured from human subjects in sensory tests. The results of experiments involving 22 odorants showed medium strength correlations between each index and perceptual similarity. In addition, when the 3 indices were combined using their Euclidean distance, we observed middle to high correlations (r = 0.65–0.79) to human perceptual similarity. We also report the results of our use of a machine learning technique to classify the odorants into a similar and dissimilar category. Although the correct rate of classification varied from 33.3% to 92.9%, these results support the feasibility of linking the glomerular responses of rats to human perception.

Key words: glomerular response, human odor perception, machine learning, rats, sensory test

Introduction

A sensory test is the most common method of evaluating odor qualities. However, as olfactory perception differs from person to person and depends on their health and testing environments, maintaining the robustness of such testing requires a number of extremely well-trained panelists (Sato 1978).

In the field of engineering, a variety of sensing systems have been developed (Persaud and Dodd 1982). Such systems generally involve the application of a neural network or multivariate statistical analysis to identify odors based on the output of a sensor array, with each sensor responding to a specific volatile odor component (Branca *et al.* 2003; Ehret *et al.* 2011). Although most conventional odor-sensing systems focus on the identification or detection of specific odors, Haddad *et al.* (2010) recently reported an important achievement in assessing odor qualities perceived by humans through predicting odorant pleasantness from the output of artificial odorant sensors. However, one limitation of using artificial sensors to predict perceptual characteristics of humans is potential gaps between artificial and biological information processing algorithms because the anatomy and physiology of the olfactory system is not fully understood.

An approach other than artificial sensors worth noting is the use of physicochemical descriptors of odorant molecules (Khan *et al.* 2007; Haddad, Khan, et al. 2008; Haddad, Lapid, et al. 2008; Saito *et al.* 2009). The definition of such descriptors is based on the number and type of atoms involved and their combination and structure within a molecule. Khan *et al.* (2007) demonstrated that odorant pleasantness can be predicted from principal component analysis using about 1600 descriptors. However, there are no guidelines for establishing a conversion algorithm between physicochemical descriptors and perception because of a lack of detailed information regarding odorant processing algorithms in biological olfactory systems, which is the same problem limiting the use of artificial odorant sensors.

In this study, we focused on systematically organizing information about the internal state of the olfactory system instead of determining information processing mechanisms. Our understanding of the mechanisms subserving odor information processing in the olfactory system reached a breakthrough with the discovery of olfactory receptor proteins and the gene family of receptors for odorant molecules (Buck and Axel 1991). Another important development was the formulation of the odor map for responses evoked on the glomerular layer of the olfactory bulb (Johnson *et al.* 1998; Mori 1999; Uchida *et al.* 2000; Mori and Sakano 2011, Falasconi *et al.* 2012). Comparing glomerular activity patterns with the behavior of rats, Youngentob *et al.* (2006) found that the activity patterns evoked on the rats' olfactory bulb are closely related to their behavior. These findings have expanded the potential for analysis of the relationships between perceptual characteristics and odorants by taking the internal states of olfactory system into consideration.

Based on this background, we herein propose a new approach for predicting olfactory perception in humans based on neural activity in the olfactory system, such that odorant qualities perceived by humans can be assessed in a more biologically natural way. In this study, it was assumed that olfactory perception characteristics are preserved to a certain extent across species, and rat activity patterns were applied to predict perceptual characteristics of humans based on previous work (Zhang and Firestein 2002; Mandairon *et al.* 2009) and the fact that the structure of the rat olfactory system (Figure 1) is similar to that of humans (Firestein 2001). As a first step, this article discusses the relationship between features extracted from glomerular activity patterns on the olfactory bulb of rats and perceptual similarity of odorants across humans to support prediction of odorant qualities.

Materials and methods

Among several sensory test protocols, evaluating the perceptual similarity to a defined standard odor is one of common protocol. For instance, in the sensory test on Japanese sake,

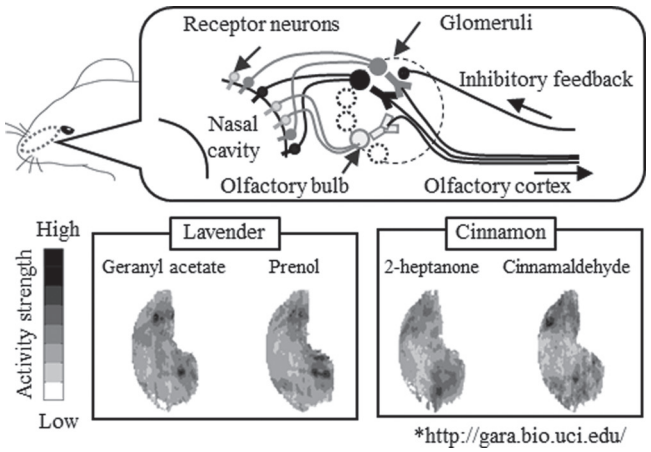

Figure 1. Illustration of the olfactory system and glomerular activity patterns. The glomeruli accumulate signals from olfactory receptor neurons expressing a particular type of receptor. The glomerular activities are then sent to the olfactory cortex via mitral and tufted cells in the olfactory bulb. Therefore, glomerular activity patterns are the basic input for further processing in the olfactory system. The lower row shows examples of glomerular activity wherein similar odor qualities evoked similar activity patterns.

a list of standard odors called the "Flavor wheel" provides a criterion for evaluation (Utsunomiya *et al.* 2006). This list also defines the odorant components in detail. Well-trained human panelists then smell the odor and determine whether the test odor contains odors defined in the Flavor wheel. As this assessment evaluates an odor in the space spanned by similarities to the standard odors, if prediction of the perceptual similarity between odors becomes possible, such a prediction method can support or replace this kind of sensory test.

This article proposes a machine learning approach for predicting the perceptual similarities of humans using glomerular activity patterns of rats. However, because there are about 2000 glomeruli, the glomerular activity patterns are high dimensional information that can cause so-called curse of dimensionality when applying machine learning technique. We thus defined 3 indices for describing the similarities between activity patterns and used them to predict perceptual similarities. To test the relationship between the defined indices and perceptual similarities, a series of sensory tests on human subjects was also conducted. This section describes the definition of these indices, the protocol of the human sensory test, and the methods used for the prediction of odor similarity.

Digitization of glomerular activity patterns

To predict perceptual similarity based on the neural representation of an odor, we focused on activity in the glomerular layer on the olfactory bulb. Johnson *et al.* (1998) measured whole glomerular activity patterns from rats using 2-deoxyglucose (2DG) and compiled an open access

database (http://gara.bio.uci.edu/). Currently, glomerular activities corresponding to about 400 kinds of odorants are available from this Web site. Glomerular activity patterns used in this article are shown in Figure 2. Although the 2DG method cannot measure dynamic responses, it provides measures of activity patterns across the whole bulbar surface. The activity patterns shown in Figure 2 are a ventral-centered view of an unrolled map of the bulbar surface provided in .png format at an image size of 197 by 357 pixels. The brightness of each pixel represents the spatial distribution of 2DG uptake normalized by z-scores relative to entire glomerular layer. A key relating brightness to z-scores is shown as a gray scale bar in Figure 3. The z-scores are linearly normalized to a range of [0, 1] from the original range of [−2, 7].

Before calculating the indices between the activity patterns, we trimmed the length of the data to obtain equally sized vectors because each activity pattern had a different shape and thus a different sized activity pattern vector. To carry out this operation, we first made a lattice filter sized of 37×86 lattices filter as shown in Figure 3, where a value of 1 denotes that it is in the glomerular layer, whereas 0 indicates that it is from the background image. The filter boundary was manually determined by tracing the glomerular shape based on a previous study (Johnson *et al.* 2002), and the number of lattices was determined based on the number of actual glomeruli. The original image size of 197 by 357 pixels was then filtered by the lattice such that about 4–5 by 5–6 pixels were assigned to the lattice. Finally, the brightness of the pixels was converted to z-values corresponding to the strength of the activity, and the strengths of the activity in the same lattice were averaged to represent the overall strength of the activity in the lattice. By extracting the strength of the activity in each part of the glomerulus with the lattice filter value of 1, T lattices of activity strength $\boldsymbol{X}_k \in \mathbb{R}^T$ were obtained ($T = 1805$ in this article).

Similarity between neural activity patterns

To evaluate the similarity between activity patterns, we defined 3 indices. The first index is the correlation between different glomerular activity patterns. The second index is the overlap rate (Xu *et al.* 2003), which describes the degree of shared strongly activated areas between different activity patterns. The third index is the degree of similarity between histograms of the strength of activity. Correlations and overlap rate were chosen because they were commonly used to evaluate topological similarity between neural activities in previous studies. For example, correlations have been employed to discuss relationships between odorant structures and neural activity (Johnson *et al.* 2002), and overlap rate has been used to determine odor maps of responses to aldehydes and esters in mice (Xu *et al.* 2003). The degree of similarity between histograms of the strength of activity was chosen to evaluate nontopological similarity, which is derived from an object image recognition technique (Bernt and Crowley 2000).

The Pearson's correlation C_{sz} between the activity pattern $\boldsymbol{X}_s$ of a standard odorant and $\boldsymbol{X}_z$ of a comparison odorant is given by the following equation:

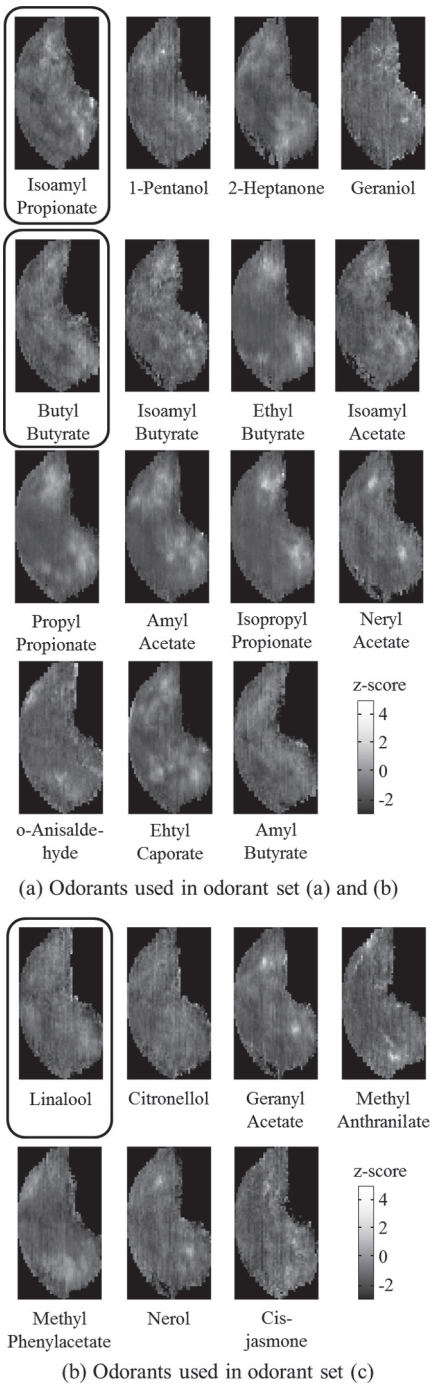

Figure 2. Glomerular activity patterns in rats that are provided at the Web site http://gara.bio.uci.edu/. Glomerular activity patterns evoked by the odorants in (a) odorant sets (a) and (b) described in Sensory tests (under Materials and methods) and (b) odorant set (c). The gray scale represents the distribution of activity strength as represented by z-scores.

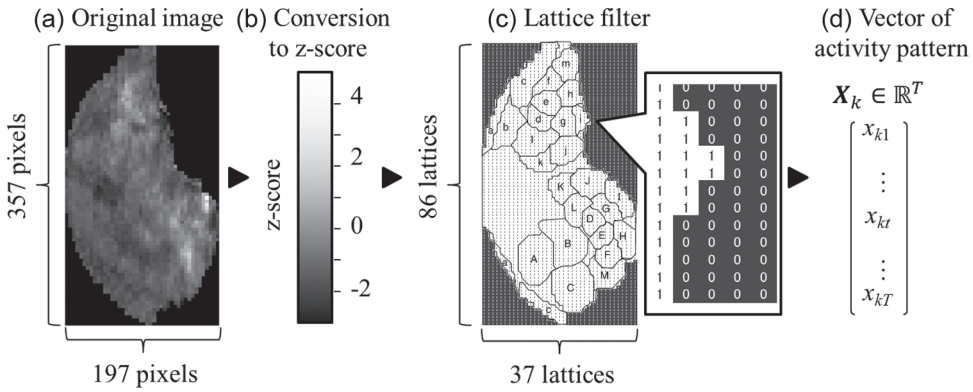

Figure 3. Digitization process for the glomerular activity pattern of *k* = isoamyl propinoate (from http://gara.bio.uci.edu). (a) The original image is a gray scale picture with a black background. (b) The brightness of each pixel converted to z-scores based on the gray scale bar shown in the Web site. (c) A lattice filter adapted on the matrix of converted z-scores to extract an equal sized activity pattern vector. The boundary of the lattice filter was determined by tracing the glomerular shape described in the literature (Johnson *et al.* 2002). Letters in the picture represent glomerular modules but that is beyond the scope of this article. (d) The calculated activity strength of all pixels *xkt* arranged as a $\boldsymbol{X}_k \in \mathbb{R}^T$ vector.

$$C_{sz} = \frac{\sum_{t=1}^{T}(x_{st} - \bar{x}_s)(x_{zt} - \bar{x}_z)}{\sqrt{\sum_{t=1}^{T}(x_{st} - \bar{x}_s)^2}\sqrt{\sum_{t=1}^{T}(x_{zt} - \bar{x}_z)^2}}, \quad (1)$$

where x_{st} and x_{zt} are the activity strength in lattice t, and $\bar{x}_s$ and $\bar{x}_z$ are the average activity strength over the activity patterns $\boldsymbol{X}_s$ and $\boldsymbol{X}_z$, respectively.

The overlap rate (O_{sz}), defined by the following equation, represents the ratio of areas common to both $\boldsymbol{X}_s$ and $\boldsymbol{X}_z$ that show strong activity in comparison to the total area:

$$O_{sz} = \frac{S(\boldsymbol{X}_s) \cap S(\boldsymbol{X}_z)}{S(\boldsymbol{X}_s)}. \quad (2)$$

The function $S(\boldsymbol{X}_s)(k \in s,z)$ is a binarized function used to calculate the position of lattices that have strong activity ($x_{kt} > \theta$).

Figure 4b shows binarized activities extracted using $S(\boldsymbol{X}_k)$ from the original images of the activity patterns shown in Figure 4a, when θ was 0.52. The degree of similarity between histograms of the strength of activity $\tilde{H}_{sz}$ was defined by the following equation:

$$\tilde{H}_{sz} = 1 - \frac{H_{sz}}{H_{max}}, \quad (3)$$

$$H_{sz} = \sum_{n=1}^{N} \frac{\left(R_n(\boldsymbol{X}_s) - R_n(\boldsymbol{X}_z)\right)^2}{R_n(\boldsymbol{X}_s) + R_n(\boldsymbol{X}_z)}, \quad (4)$$

where $R_n(\boldsymbol{X}_k)$ is the number of lattices in a range of activity strengths of $R_n = [b_{n-1}, b_n]$ (n = 1, 2, 3, …, N) included in a given activity pattern $\boldsymbol{X}_k$, where b is the bin size of the activity strength and $N = 1/b$ is the total number of bins.

Figure 4d shows histograms of the strength of activity calculated from original images of the activity patterns (Figure 4a), with a step size b = 0.05 and N = 20. Here, H_{max} is the maximum value of H_{sz} in an odorant set, as described in Sensory tests (under Materials and methods). The parameters used for the 3 indices were θ and b, as defined above. In this article, these parameters were empirically determined to yield the best correlations of perceptual similarities across odorants.

Sensory tests

To obtain the perceptual characteristics of human subjects, we asked human subjects to smell odorants absorbed on a paper odor stick enclosed in a zipper bag and asked them to rate the perceptual similarities between a set of comparison odorants and a standard odorant. Based on previous sensory test procedure (Le Berre *et al.* 2007; Perrin *et al.* 2008), the sensory test task was arranged in 2 phases assuming that the subjects do not have specialized skills for odor evaluation, and that the odorants presented are novel to the subjects. Because memorizing the qualities of the odorants and completing the comparison task would be very difficult for untrained subjects (Kaeppler and Mueller 2013), in the first phase of sensory test, we asked the subjects to smell the odorants freely and repeatedly to facilitate the subjects getting familiar with the odorants. In the second phase, a standard odorant was presented, and the subjects smelled other comparison odorants and categorized the odorants as similar or dissimilar to a standard odor. This forced-choice, similar/dissimilar task was used because our pilot experiments indicated that subjects had difficulty rating the odorants using an analog scale.

It should be noted that the experimental conditions used with the rats (Johnson *et al.* 2002) and the sensory test performed in this article are different. First, the odorant concentrations were not strictly controlled in our task.

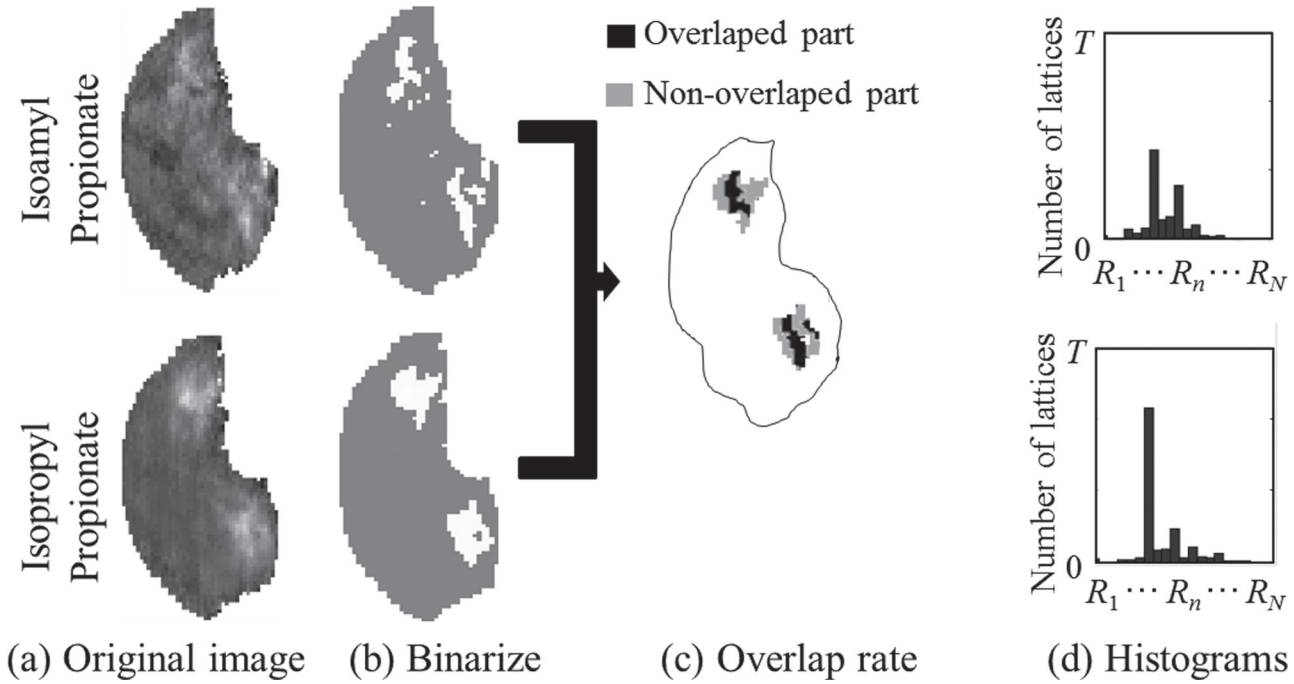

Figure 4. Examples of overlap rate and histograms of the strength of activity. (a) Glomerular activity patterns evoked by isoamyl propionate and isopropyl propionate; (b) binarized activity, $S(Xk)$; and (c) the area of overlap (in black) when isopropyl propionate is the standard activity pattern, X_s; (d) histograms of the strength of activity showing the complexity of the distribution of activity.

This was designed to reduce the burden on the subjects—by, for example, eliminating the need for constraint to any particular delivery device—and obtain perceptual characteristics as spontaneously as possible. The presented odorants were diluted using mineral oil (Yamamoto Yakuhin Co., Ltd, Hiroshima, Japan) on neat odorants to achieve as matched an intensity across odorants as possible. Before performing the sensory test, the intensity of the odorants was rated by subjects different from those who performed the sensory test. Conversely, in the rat experiments, saturated vapors over neat odorant were diluted using ultrazero grade air. The odorants used in the experiments and their dilution factors are shown in Table 1. Second, we did not match the odorant concentration between humans and rats because that likely does not guarantee equal odor intensities because of species differences. The rats were exposed to the smell odorant for about 45 min under a constant odorant concentration, whereas the humans could freely and repeatedly smell the odor stick, and the odorant concentration conveyed to the nasal cavity could vary according to the smelling behavior of the subject.

The odorants were chosen based on the odor descriptors described along with the glomerular activity patterns on the Web site http://gara.bio.uci.edu/ as shown in Table 1. The criterion for choosing an odorant was that subjects do not report that it smells bad; therefore, we chose odorants with descriptors such as "banana" or "sweet." A second criterion was that there are a sufficient number of odorants that share the same descriptors as the chosen odorant, which could be used as comparison odorants, because it is difficult to find pairs of single-component odorants that smell similar.

The above protocol was approved by the ethics committee (epidemiological study) of Hiroshima University, Hiroshima, Japan, for experimentation on human subjects. It complies with the Declaration of Helsinki for Medical Research involving Human Subjects. All subjects provided written informed consent to participate in the test. The details of the sensory test procedures are described below:

Phase 1: Memorizing odorants

1. Subjects smelled a standard odorant (shown in Table 1) to memorize its smell.
2. Subjects rested for 90 s outside the examination room to prevent odor fatigue and to allow for indoor ventilation.
3. Subjects were presented with 6 odorants, consisting of a fixed group and odorant group 1–4 (Table 1). The fixed group was always presented in the subsequent phase to stabilize the ratings of other odor sets and thereby reduce the variance in the rating data.
4. Subjects rested for 90 s outside the examination room to prevent odor fatigue and to allow for indoor ventilation.

Phase 2: Similarity evaluation

5. Subjects were presented with the 6 comparison odorants and were asked to select those odorants that smelled

Table 1 Sets of odorant used in the sensory testing

Presenting set	Odorant name (abbreviation)	Dilution factor (human)	Dilution factor (rat)	Odor descriptors	Literature
(a) Odorant set (a)					
Fixed group	1-Pentanol (1P)	1/120	1/110	Fusel, sweet	Johnson *et al.* (2004)
	2-Heptanone (2H)	1/80	1/29	Fruity, spicy, cinnamon, banana	Johnson *et al.* (2004)
	Geraniol (G)	1/20	1/8	Sweet, rose, woody, floral	Johnson *et al.* (2002)
Group 1	Amyl butyrate (AB)	1/20	1/10	Banana	http://gara.bio.uci.edu
	Butyl butyrate (BB)	1/10	1/10	Banana	http://gara.bio.uci.edu
	Isoamyl butyrate (IB)	1/10	1/14	Fruity, apricot, pineapple, banana	Johnson *et al.* (1998)
Group 2	Ethyl butyrate (EB)	1/50	1/225	Banana, pineapple, berry, cognac	Johnson *et al.* (2004)
	Isoamyl acetate (IA)	1/40	1/91	Fruity, banana, sweet, solvent	Johnson *et al.* (2002)
	Propyl propionate (PP)	1/40	1/224	Fruity, floral, apple, pineapple	Johnson *et al.* (2005)
Group 3	Amyl acetate (AA)	1/50	1/72	Banana, pear, sweet, fruity	Johnson *et al.* (2005)
	Isopropyl propionate (IPP)	1/40	1/395	Fruity, sweet, pineapple, banana	Johnson *et al.* (2005)
	Neryl acetate (NA)	1/5	1/8	Orange blossom, rose, sweet, fruity	Johnson *et al.* (2007)
Group 4	o-Anisaldehyde (oA)	1/30	a	Phenolic, sweet, balsam, floral	Johnson *et al.* (2002)
	Ethyl caproate (EC)	1/50	1/21	Wine, apple, banana, brandy	Johnson *et al.* (2004)
	Amyl butyrate (AB)	1/20	1/10	Banana	http://gara.bio.uci.edu
Standard	Isoamyl propionate(IP)	1/20	1/87	Banana	http://gara.bio.uci.edu
(b) Odorant set (b)					
Fixed group	1-Pentanol (1P)	1/120	1/110	Fusel, sweet	Johnson *et al.* (2004)
	2-Heptanone (2H)	1/80	1/29	Fruity, spicy, cinnamon, banana	Johnson *et al.* (2004)
	Geraniol (G)	1/20	1/8	Sweet, rose, woody, floral	Johnson *et al.* (2002)
Group 1	Amyl butyrate (AB)	1/20	1/10	Banana	http://gara.bio.uci.edu
	Isoamyl propionate (IP)	1/20	1/10	Banana	http://gara.bio.uci.edu
	Isoamyl butyrate (IB)	1/10	1/14	Fruity, apricot, pineapple, banana	Johnson *et al.* (1998)
Group 2	Ethyl butyrate (EB)	1/50	1/225	Banana, pineapple, berry, cognac	Johnson *et al.* (2004)
	Isoamyl acetate (IA)	1/40	1/91	Fruity, banana, sweet, solvent	Johnson *et al.* (2002)
	Propyl propionate (PP)	1/40	1/224	Fruity, floral, apple, pineapple	Johnson *et al.* (2005)
Group 3	Amyl acetate (AA)	1/50	1/72	Banana, pear, sweet, fruity	Johnson *et al.* 2005
	Isopropyl propionate (IPP)	1/40	1/395	Fruity, sweet, pineapple, banana	Johnson *et al.* (2005)
	Neryl acetate (NA)	1/5	1/8	Orange blossom, rose, sweet, fruity	Johnson *et al.* (2007)

Table 1 Continued

Presenting set	Odorant name (abbreviation)	Dilution factor (human)	Dilution factor (rat)	Odor descriptors	Literature
Group 4	o-Anisaldehyde (oA)	1/30	a	Phenolic, sweet, balsam, floral	Johnson *et al.* (2002)
	Ethyl caproate (EC)	1/50	1/21	Wine, apple, banana, brandy	Johnson *et al.* (2004)
	Amyl butyrate (AB)	1/20	1/10	Banana	http://gara.bio.uci.edu
Standard	Butyl butyrate (BB)	1/10	1/10	Banana	http://gara.bio.uci.edu
(c) Odorant set (c)					
Fixed group	Cis-Jasmone (CJ)	1/10	1/8	Floral, woody, jasmine, citrus	http://gara.bio.uci.edu
	Citronellol (CI)	1/20	1/36	Rose, floral, petal, waxy	Johnson *et al.* (2007)
	Geranyl acetate (GA)	1/10	1/8	Rose, lavender, sweet, floral	Johnson *et al.* (2007)
	Methyl anthranilate (MA)	1/10	1/8	Orange blossom, jasmine, musty, fruity	Johnson *et al.* (2005)
Group 1	Methyl anthranilate (MA)	1/10	1/8	Orange blossom, jasmine, musty, fruity	Johnson *et al.* (2005)
	Methyl phenylacetate (MP)	1/10	1/9.9	Sweet, honey, jasmine, fruity	Farahbod *et al.* (2006)
	Nerol (N)	1/10	1/8	Sweet, rose, neroli, citrus	Johnson *et al.* (2007)
Standard	Linalool (L)	1/30	1/45	Orange, sweet, bergamot, lavender	http://gara.bio.uci.edu

[a]1/8 dilution of saturated vapor over a 1/10 dilution of the neat material in a 95% ethanol dilution of saturated vapor over the neat material.

similar to the standard odor. This experiment was performed under the following conditions:

- Odorants were presented using a zipper bag containing a paper odor stick. The odor stick was dipped into the appropriate odor oil before the experiment.
- Subjects could smell the odors at any time, and there was no limitation on repeated smelling of the presented odors.

The odorant group, except the fixed group, was changed, and steps 1–5 were repeated until the subjects completed the evaluation of all test odorants. This test was thus conducted 4 times for odorant set (a) and (b) and 1 time for odorant set (c). Six subjects (college students) in their twenties participated in the tests. The sensory test for each odorant set (Table 1) was performed on different days for each subject.

We recorded a score of 1 when the comparison odor was judged to be "similar" to the standard odor and 0 when the comparison odor was judged to be "dissimilar." The perceptual similarity, D, between odorants was defined as the proportion of total ratings that were rated as "1."

Predictors of perceptual similarity

First, the Euclidean distance among the 3 indices were defined as the degree of difference between activity patterns related to the standard odorant and those related to the comparison odorants. Because the indices are $C_{sz} = O_{sz} = \tilde{H}_{sz} = 1$ when a glomerular activity pattern is exactly the same as that of standard odorant, dissimilarity between the activity patterns related to the standard odorant and those related to the comparison odorants was defined as

$$e_{sz} = \sqrt{\left(1 - C_{sz}\right)^2 + \left(1 - O_{sz}\right)^2 + \left(1 - \tilde{H}_{sz}\right)^2}. \quad (5)$$

We then investigated the relationship between this glomerular activity pattern–based Euclidean distance and perceptual similarity, D.

Subsequently, predictions of similarities for all odorants were carried out using the log-linearized Gaussian mixture network (LLGMN; Tsuji *et al.* 1999). LLGMN expands the Gaussian mixture model to a neural network using a log-linearized method to approximate the probability density function (pdf) of the output vector on the input vector space and enables estimation of a posteriori probability of each class Y^m ($m = 1, \ldots, M$; M is the number of classes) given an

input vector. The following details the structure and configurations of the LLGMN used in this article.

In this article, we classified the 3 similarity indices $\boldsymbol{u} = [C_{sz}, O_{sz}, H_{sz}]^T$ calculated from a pair of glomerular activity patterns into $K = 2$ classes ($k = 1$, similar; $k = 2$, dissimilar). A similar odorant to the standard odorant was defined as the perceptual similarity $D > T_D$, whereas a dissimilar odorant was defined as $D \leq T_D$. If $M = 2$, Gaussian components were used to approximate the pdf for each class, the structure of the LLGMN can be determined, as shown in Figure 5. First, the LLGMN nonlinearly transforms the input vector $\boldsymbol{u} \in \mathbb{R}^3$ by

$$\boldsymbol{U} = \left[1, \boldsymbol{C}_{sz}, \boldsymbol{O}_{sz}, \boldsymbol{H}_{sz}, \boldsymbol{C}_{sz}^2, \boldsymbol{C}_{sz}\boldsymbol{O}_{sz}, \boldsymbol{O}_{sz}^2, \boldsymbol{O}_{sz}\boldsymbol{H}_{sz}, \boldsymbol{H}_{sz}^2 \right]^{\mathrm{T}} \in \mathbb{R}^{10}, \quad (6)$$

where each element of $\boldsymbol{U}$ is in a range of [0, 1] based on its definition in "Similarity between neural activity patterns". The weights connecting the first layer to the second layer represent the parameters included in the Gaussian mixture model, but they are mixed because of the log linearization. The second layer consists of $KM = 4$ Gaussian component units and each unit determines the m-th Gaussian distribution in a class k based on the weights connecting the first layer. The a posteriori probability of a m-th Gaussian distribution in a class k was calculated in this layer if an appropriate set of weight parameters was acquired. The unit in the second layer that belongs to class k is connected to the k-th unit in the output layer. The output layer consists of $K = 2$ units, which estimates the a posteriori probability of a class k by summing up the output of units in the second layer. Here, the only parameter that has to be configured to determine the structure of LLGMN is the

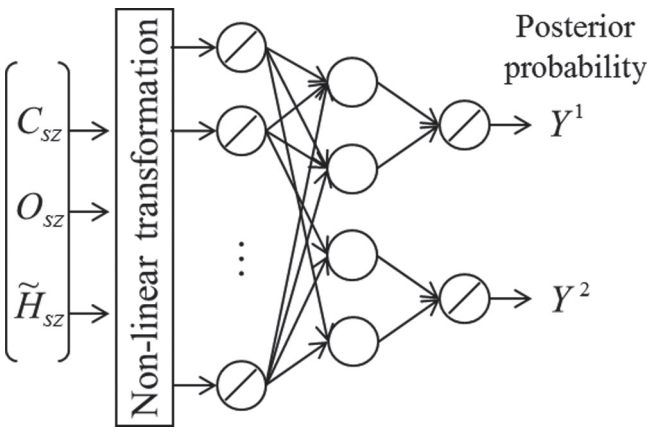

Figure 5. Structure of the log-linearized Gaussian mixture network (LLGMN; Tsuji *et al.* 1999). The input vector was composed of 3 indices as defined in Similarity between neural activity patterns. The network allows estimation for posterior probabilities of similar Y^1 and nonsimilar odors Y^2 for a given input vector. The network is composed of an input layer with 10 units, a second layer with 4 units, and an output layer with 2 units each corresponding to similar and nonsimilar classes.

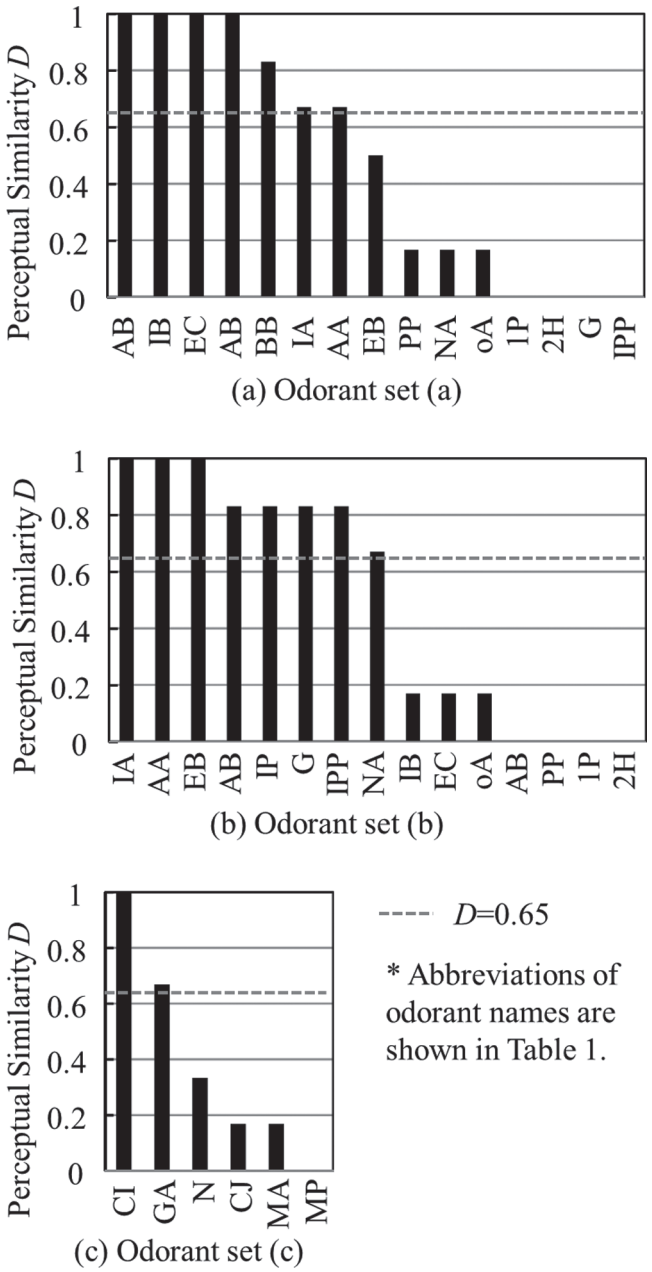

Figure 6. Perceptual similarity obtained from the sensory tests. The *x* axis represents comparison odorants and the *y* axis represents the rated perceptual similarity *D* between the comparison odorants and the standard odorant. Odorants are represented by the abbreviations shown in Table 1 and arranged in descending order of *D*. The gray dotted line in each figure denotes $D = 0.65$. The odorants above this line were rated as similar to the standard odorant by the majority of subjects. (a) Odorant set (a), (b) odorant set (b), and (c) odorant set (c).

Gaussian component number m. This parameter was empirically set based on the complexity of the distribution of input vector $\boldsymbol{u}$.

Provided with the structure of the LLGMN described above, the weights between the first and second layer were optimized. Before performing the weight adjustment, a learning data set consisting of pairs of input vectors $\boldsymbol{u}$ and

corresponding teaching vectors $\boldsymbol{T}^{(n)} = (T_k^{(n)}) \in \mathbb{R}^k$ was collected, and the weights in the LLGMN were initialized as small numbers ($\ll 1$). The elements of the teaching vector were set to $T_k^{(n)} = 1$, if the sample input vector belongs to class k otherwise $T_k^{(n)} = 0$. For example, if an input vector belongs to a similar odorant (k = 1), then $\boldsymbol{T}^{(n)} = [1,0]^T$, and if it belongs to dissimilar odorant, then $\boldsymbol{T}^{(n)} = [0,1]^T$. Using these sample data sets, the LLGMN automatically adjusts the parameters based on a back propagation algorithm minimizing the following evaluation function:

$$J = -\sum_{n=1}^{N}\sum_{k=1}^{K} T_k^{(n)} \log Y^k, \tag{7}$$

where Y^k is the output of the k-th unit in the output layer. The prediction procedure was carried out using a leave-one-out method, where the parameters involved in the LLGMN were adjusted using all available data sets except one prediction target odorant. Predictions of perceptual similarity were then performed by feeding prediction target odorants into the LLGMN. Discrimination results were defined as a class with the maximum posterior probability calculated by the LLGMN. The prediction target odorant was methodically changed until predictions were completed for all comparison odorants. Finally, the accuracy of the predictions for all odorants used in the sensory test was evaluated, as shown in Table 1.

Results and discussion

This section reports the results of the sensory tests performed using the protocol described in Sensory tests (under Materials and methods). The obtained perceptual similarities were compared with the 3 indices described in Similarity between neural activity patterns. Finally, we used the LLGMN described in Predictors of perceptual similarity to predict perceptual similarity based on the 3 indices. The parameter dependency of the 3 indices and effects of concentration on the accuracy of these indices as predictors of odorant perception are also discussed in this section.

Sensory tests

The tests described in Sensory tests (under Materials and methods) were performed on 6 subjects for each odorant set shown in Table 1. The perceptual similarity D between the comparison odorants and the standard odorant are shown in Figure 6. Using the criterion for perceptual similarity, as D higher than T_D = 0.65, 6 corresponding odorants were classified as similar odorants for odorant set (a), 7 for odorant set (b), and 2 for odorant set (c). T_D = 0.65 means that majority of the subjects (4 or more out of 6) judged the comparison odorant to be similar to the standard odorant.

Note that odorant sets (a) and (b) were composed of the same comparison odorants but different standard odorants, which were isoamyl propionate for odorant set (a) and butyl butyrate for odorant set (b). This was aimed at investigating the influence of the standard odor on perceptual similarity. From the results of the sensory test, we confirmed that both standard odorants smelled similar to each other. Among the 7 odorants that smelled similar to butyl butyrate (D > 0.65 in odorant set (b)), 6 odorants were also similar to isoamyl propionate. This finding suggests that the choice of standard odorant had minimal effects on perceptual characteristics in this sensory test task. In addition, group 1 and 4 in the both odorant set (a) and (b) contain a common comparison odorant amyl butyrate. This is aimed to test how the choice of odorant group influences the subject's decision. The result confirmed that there was no subject changed decision

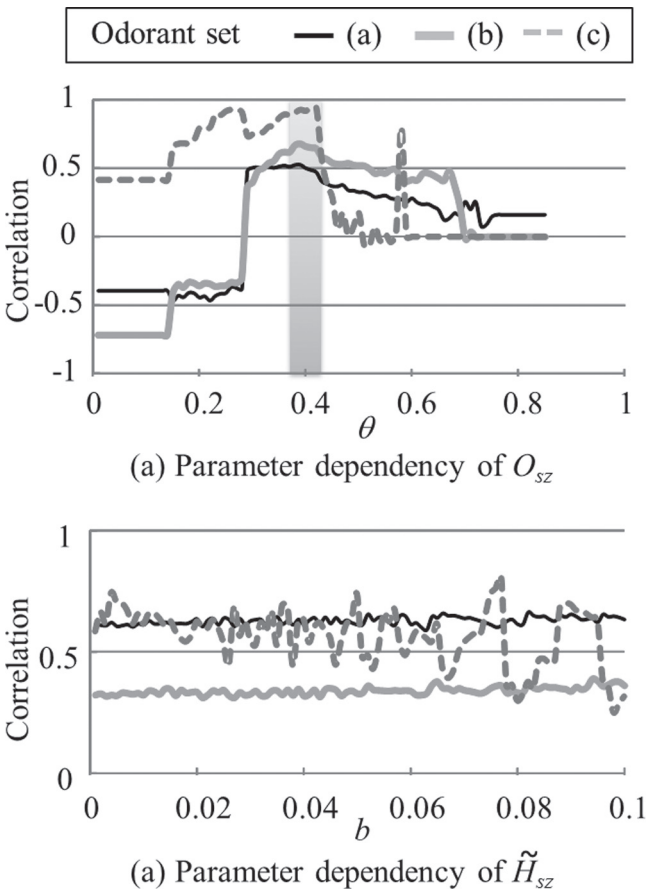

Figure 7. Parameter dependencies of the indices. The solid black line shows the results collected with odorant set (a), the gray solid line designates the results for odorant set (b), and the dotted gray line designates the results for odorant set (c). (a) The correlation between the overlap rate O_{sz} and perceptual similarity D calculated under different binarized threshold θ. A gray background demonstrates a rough range of θ yielding the highest correlation. The lines are truncated at approximately θ > 0.85 because there were no overlapping areas for these parameters. (b) Correlation between histograms of the strength of activity $\tilde{H}_{sz}$ and the perceptual similarity D calculated under different bin sizes for histogram b. There was no obvious correlation; however, lower b values yielded more reliable correlations with D.

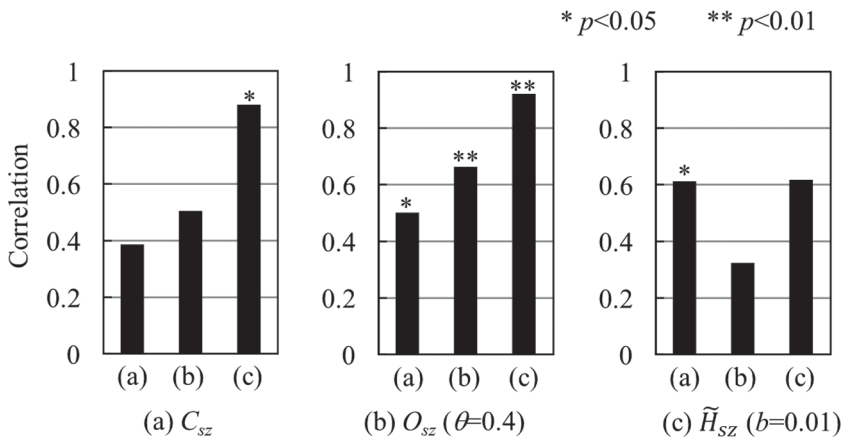

Figure 8. Correlation between the indices examined and perceptual similarity *D*. The *x* axis represents odorant set, and the *y* axis shows the corresponding correlation. (a) Performance of the index C_{sz} calculated between glomerular activity pattern of the standard odorant and comparison odorants, (b) the overlap rate O_{sz} between the activity patterns when the parameter θ was set to 0.4, and (c) the similarity between histograms of the activity patterns $\tilde{H}_{sz}$. Middle to high correlations between the indices and perceptual similarity were observed.

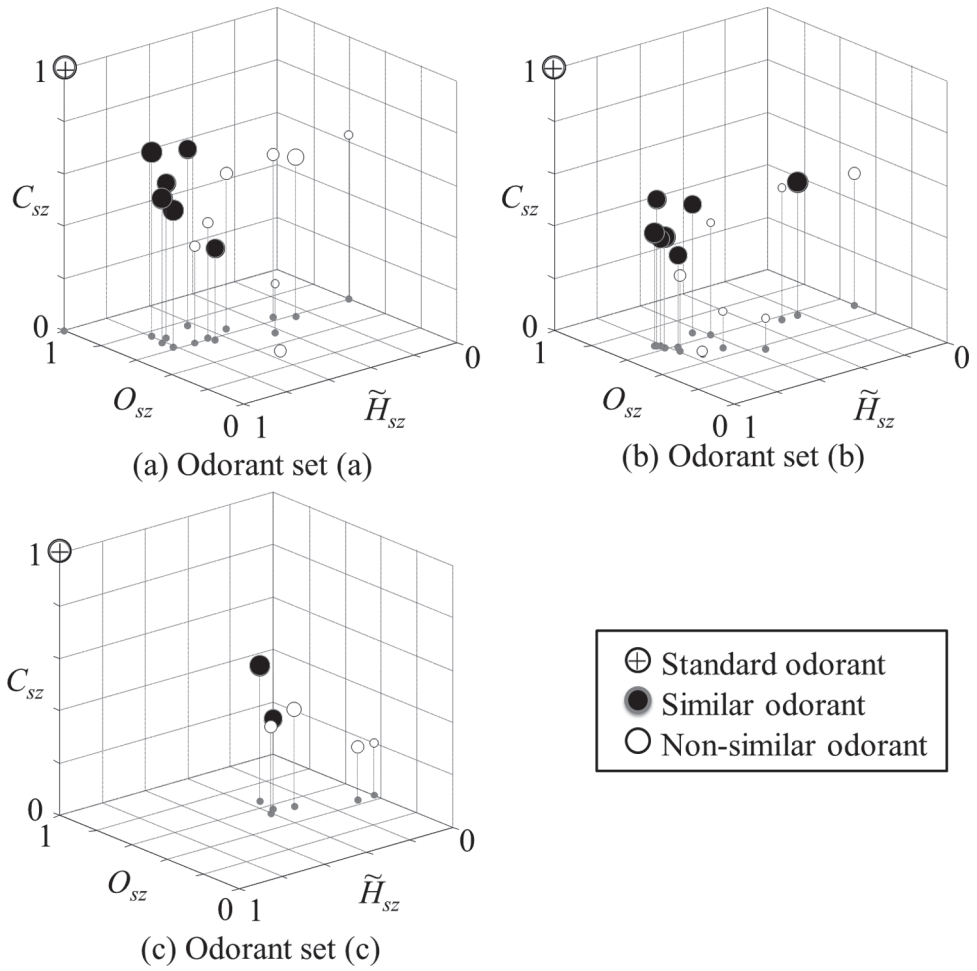

Figure 9. Distribution of odorant in the space spanned by the 3 indices (correlation C_{sz}, overlap rate O_{sz}, and similarity between histograms $\tilde{H}_{sz}$). The radius of each circle is scaled relative to the perceptual similarity *D*. Black circles denote odorants with a similarity of $D > 0.65$, whereas white circles denote those with a lower similarity to the standard odorant. The drop-down lines from each point anchor the point on the O_{sz}–$\tilde{H}_{sz}$ plane. Odorants with higher similarity tended to be distributed closer to the standard (upper left side) for all odorant sets.

between two odorant groups that amyl butyrate is similar to the standard odorant. These results can be contributed by including a fixed group in all comparison groups to maintain judgment criteria of the subjects. The sensory test protocol thus could stabilize intrasubject variability.

Comparison between perceptual similarity and activity patterns

Relationships between perceptual similarity D obtained from the sensory tests and the 3 indices based on glomerular activity patterns (the correlation coefficient, C_{sz}, the overlap rate, O_{sz}, and the degree of similarity between histograms of the strength of activity, $\tilde{H}_{sz}$) were examined. Because parameters θ and b have to be determined for calculating O_{sz} and $\tilde{H}_{sz}$, parameters that yield the highest correlation with perceptual similarity were explored. Parameter θ was examined in a range of [0, 1] by step size of 0.01. The results shown in Figure 7a indicate that the highest correlation can be achieved around θ = 0.4 for all odorant sets. In the same manner, parameter b was examined in a range of [0, 0.1] by step size of 0.001. The results shown in Figure 7b suggest that the similarity of histogram of the strength of activity $\tilde{H}_{sz}$ only minimally depends on the bin size b. However, when the bin size b is large, a small change in b results in unpredictable changes in performance of $\tilde{H}_{sz}$. Based on the above results, the parameters chosen were θ = 0.4 and b = 0.01. Figure 8 shows the performance of the indices using these parameters. We observed middle to high correlations between the indices (C_{sz}, O_{sz}, $\tilde{H}_{sz}$) and perceptual similarity D for all odorant sets (a), (b), and (c).

Furthermore, we plotted comparison odors on a 3-dimensional graph using the 3 indices. Figure 9 shows the plot where the x axis is the overlap rate O_{sz}, the y axis is the similarity between $\tilde{H}_{sz}$, and the z axis is the correlation coefficient C_{sz}. The diameter of the circles corresponds to the perceptual similarity D obtained from the sensory tests. The black circles indicate those odorants for which the perceptual similarity D was $T_D > 0.65$, whereas the white circles indicate those odorants for which the perceptual similarity was $D \leq 0.65$. From Figure 9, we can see that those odorants that were similar to a standard odorant were distributed largely on the upper left side compared with those with a lower perceptual similarity to a standard odorant. Figure 10a plots the Euclidean distance e_{sz} on the x axis and the perceptual similarity D on the y axis for each odorant set. These figures confirm that a middle to high correlation exists between the Euclidean distance e_{sz} and perceptual similarity D, indicating that glomerular activity patterns in rats predict perceptual characteristics in humans.

Finally, we compared the performance of the Euclidean distance of the 3 indices with that calculated from the physicochemical descriptors of odorants reported in a previous study. Haddad, Khan, et al. (2008) reported that the perceptual similarity between odorants correlates, to a certain degree, with the Euclidean distance of physicochemical descriptors. To compare the proposed approach to the previous method, we calculated 1592 different physicochemical descriptors available for the 22 odorants used in the sensory tests and performed principal component analysis.

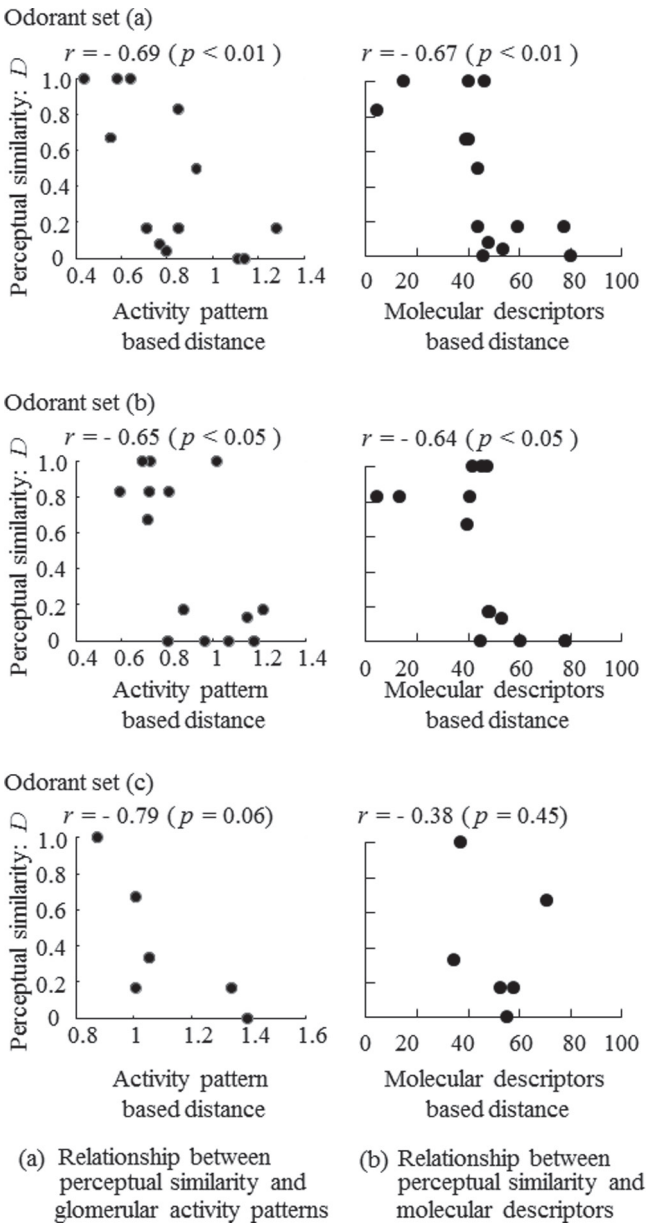

Figure 10. Relationships between perceptual similarity of the odorants and the Euclidean distance between the 3 indices. (a) The relationship between perceptual similarity D and the Euclidean distance between the standard odorant and the comparison odors in the 3-dimensional space shown in Figure 9. This figure demonstrates that the odorants with shorter Euclidean distances to the standard odorant tended to exhibit higher perceptual similarity. (b) The relationship between perceptual similarity and Euclidean distance as calculated from molecular descriptors based on a previously proposed method (Haddad, Khan, et al. 2008). Comparison of the correlations obtained from (a) and (b) shows that activity patterns can provide equivalent or higher levels of information to human perceptual ratings.

The Euclidean distances to the *n* principal components (PCs) of the physicochemical descriptors were then calculated between the standard odorant and the comparison odorants. These procedures were performed in the same manner as in a previously described method, namely, by means of the physicochemical calculation software Dragon 6 (Affinity Science, Tokyo, Japan; Talete srl, 2011) and the statistical analysis toolbox in Matlab (Mathworks, Tokyo, Japan). Figure 10b shows comparison results between perceptual similarity *D* and the physicochemical descriptor–based Euclidean distances using 4 PCs. Figure 10b, a medium correlation is apparent. Analysis of odorant set (c) demonstrated that the proposed approach yielded a much higher correlation ($r = -0.79$, $P = 0.06$) than the previous method ($r = -0.38$, $P = 0.45$). It should be noted, however, that the *P* values were relatively high for both methods. Figure 11 shows the correlation between perceptual similarity *D* and physicochemical descriptor–based Euclidean distances calculated using different numbers of PCs. The *x* axis is the number of principal components employed, and the *y* axis shows the correlation with *D*. This figure indicates that the performance of physicochemical descriptor–based Euclidean distance does not show much improvement with the use of more than 4 PCs. The results shown in Figures 10 and 11 thus indicate that the proposed approach has equivalent or higher performance to the previous method.

To investigate the reasons for the clear differences between the proposed method and the previous method we observed using odorant set (c), where the standard odor was linalool (Figure 10). We examined the molecular structure and glomerular activity pattern of an odorant included in odorant set (c). Figure 12a,b shows the activity patterns and molecular structures of the standard odorant (linalool) and a comparison odorant (geranyl acetate) that showed a

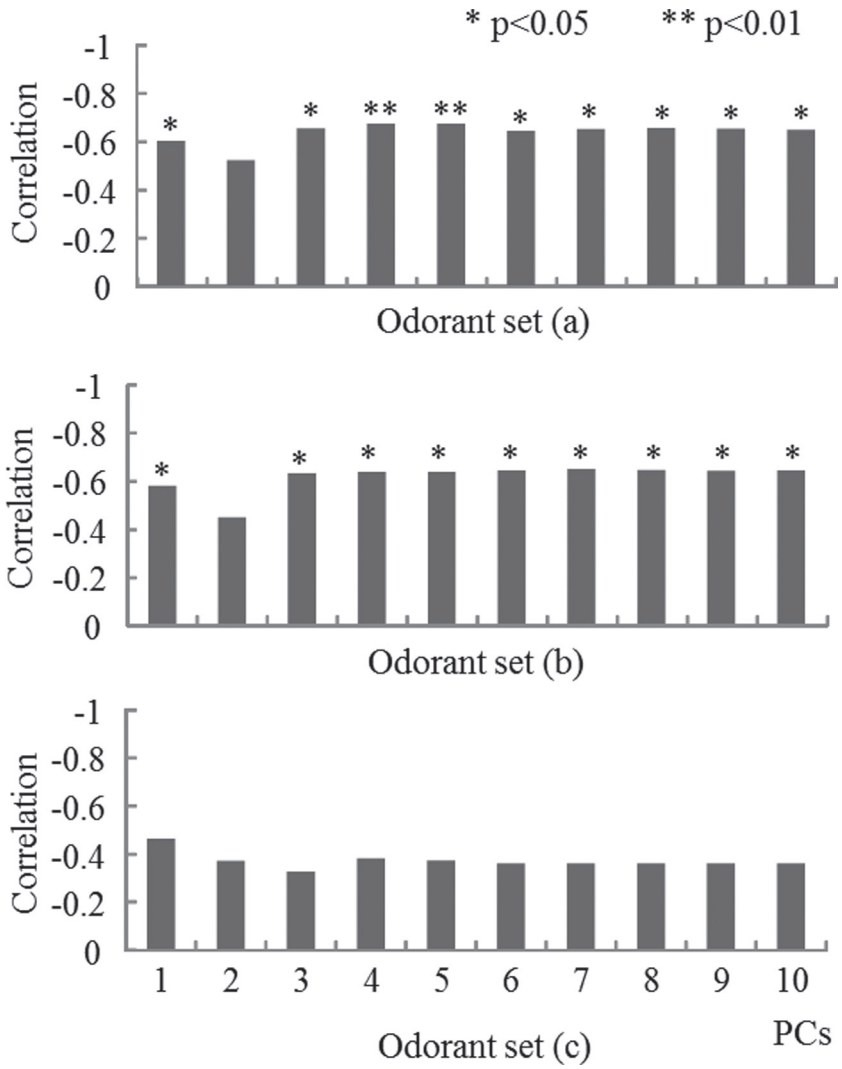

Figure 11. Correlation between perceptual similarities and physicochemical descriptor–based Euclidean distances calculated from a different number of principal components (PCs). The *x* axis represents the number of PCs and the *y* axis represents the correlation. Since the Euclidean distance indicated differences between the odorants, the correlation had a negative value. Increasing the number of PCs beyond 4 did not improve the correlation.

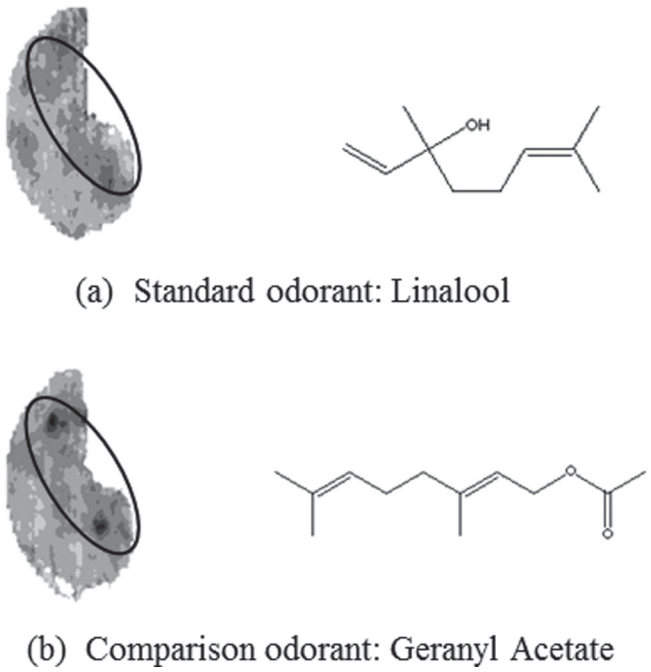

Figure 12. Glomerular activity patterns and chemical structures of the (a) standard odorant linalool and (b) that of the comparison odorant geranyl acetate with a smell similar to that of the standard odorant. To facilitate visual comparison, gray scale contrast was changed from Figure 2. Comparing (a) and (b), it can be observed that the activity patterns are similar even though the molecular structures differ.

high perceptual similarity. Figure 12a,b shows that geranyl acetate and linalool have different functional groups and branching structures. These differences may nonlinearly map to information processing in the olfactory system and yield similar glomerular activity patterns. Perceptual similarity thus became difficult to predict using a linear Euclidean distance based on physicochemical descriptors.

Predictors of perceptual similarity

The comparison results described above imply that the perceptual similarity between a pair of odorants is predictable by the extracted indices. However, because the Euclidean distance linearly combines the 3 indices with the same weight, it can only evaluate the linear relationships between perceptual similarity and the indices. We thus applied a LLGMN (Tsuji *et al.* 1999) that can produce an optimal classification plane in the space of 3 indices to predict the perceptual similarity of odorants. The threshold T_D for odorants that are similar to the standard odorant was defined as $T_D = 0.65$ as described in Sensory tests (under Results and discussion).

Table 2a and 2b shows the prediction results of the LLGMN for each odorant set. The second row contains the prediction results of the LLGMN, and the third row starting at the left shows the results of the sensory test where 0 denotes a dissimilar odorant ($D \leq 65$) and 1 denotes a similar odorant ($D > 0.65$). In the table, successful predictions are

Table 2a Classification results using a log-linearized Gaussian mixture network: Odorant set (a)

Standard odorant: Isoamyl propionate(IP)	Perceptual similarity	LLGMN[a]	LLGMN[b]
1-Pentanol (1P)	0	0	0
2-Heptanone (2H)	0	0	1
Geraniol (G)	0	1	0
Amyl butyrate (AB)	1	1	1
Butyl butyrate (BB)	1	0	1
Isoamyl butyrate (IB)	1	1	1
Ethyl butyrate (EB)	0	0	0
Isoamyl acetate (IA)	1	1	1
Propyl propionate (PP)	0	1	0
Amyl acetate (AA)	1	1	1
Isopropyl propionate (IPP)	0	0	0
Neryl acetate (NA)	0	0	0
o-Anisaldehyde (oA)	0	0	0
Ethyl caproate (EC)	1	1	1
Prediction accuracy (%)		78.60	92.90
Accuracy to the training data (%)		100	

Correct; 0: Dissimilar; 1: Similar.
[a]Using glomerular activity patterns evoked by isoamyl propionate diluted to 1/87 of saturated vapor over the neat material.
[b]Using glomerular activity patterns evoked by isoamyl propionate diluted to 1/10 of saturated vapor over the neat material.

shown by a gray background behind the odorant name. The prediction accuracies for odorant sets (a), (b), and (c) were 78.6%, 64.3%, and 33.3%, respectively.

Because we did not match the odorant concentration between human and rats, and the odorant concentration was not strictly controlled in the sensory test, we examined the effects of concentration on the performance of the LLGMN. We measured changes in the activity patterns associated with the standard odorant (isoamyl propionate and butyl butyrate) under different concentrations and performed predictions of perceptual similarities. The predicted results are shown in the fourth row from the left of Table 2a and 2b. As a result, prediction accuracy of 92.9% and 78.6% were obtained respectively for odorant sets (a) and (b). Although the effects of concentration were not negligible, the above results strongly support the possibility of predicting perceptual similarity between odorants using glomerular activity patterns in rats. Relatively small changes in the correct rate can be obtained using a concentration normalization function in the olfactory bulb. A simulation study reported that the glomerulus normalizes odorant concentration through interactions between several kinds of neurons in the olfactory bulb (Cleland *et al.* 2007). Possibly as a result, interodorant differences in neural activity patterns were larger than intraodorant differences.

Table 2b Classification results using a log-linearized Gaussian mixture network: Odorant set (b)

Standard odorant: Butyl butyrate (BB)	Perceptual similarity	LLGMN[a]	LLGMN[b]
1-Pentanol (1P)	0	0	0
2-Heptanone (2H)	0	1	0
Geraniol (G)	0	0	0
Amyl butyrate (AB)	1	1	1
Isoamyl propionate (IP)	1	0	1
Isoamyl butyrate (IB)	1	1	1
Ethyl butyrate (EB)	1	0	0
Isoamyl acetate (IA)	1	1	1
Propyl propionate (PP)	0	1	1
Amyl acetate (AA)	1	1	1
Isopropyl propionate (IPP)	0	1	0
Neryl acetate (NA)	0	0	1
o-Anisaldehyde (oA)	0	0	0
Ethyl caproate (EC)	1	1	1
Prediction accuracy (%)		64.3	78.60
Accuracy to the training data (%)		100	

[a]Using glomerular activity patterns evoked by butyl butyrate diluted to 1/10 of saturated vapor over the neat material
[b]Using glomerular activity patterns evoked by butyl butyrate diluted to 1/190 of saturated vapor over the neat material

Correct; 0: Dissimilar; 1: Similar.

Table 2c Classification results using a log-linearized Gaussian mixture network: Odorant set (c)

Standard odorant: Lialool (Li)	Perceptual similarity	LLGMN
Citronellol (CI)	1	0
Geranyl acetate (GA)	1	0
Nerol (N)	0	1
Cis-Jasmone (CJ)	0	1
Methyl anthranilate (MA)	0	0
Methyl phenylacetate (MP)	0	0
Prediction accuracy (%)		33.3
Accuracy to the training data (%)		100

Correct; 0: Dissimilar; 1: Similar.

The reason for the low prediction accuracy for odorant set (c) (Table 2c) is because most activity patterns in odorant set (c) shown in Figure 2b have broad and sporadic responses, especially that of the standard odorant linalool. Because of this feature of the 3 indices (C_{sz}, O_{sz}, $\tilde{H}_{sz}$), comparisons between odorants and standard odorants tend to yield a small value. As a result of the small range of values of the indices (Figure 9), determining the proper boundary plane separating similar and dissimilar odorants was difficult. This difficulty may arise from the fact that the defined indices only reflect spatial features of the glomerular activities. The relationships between perceptual characteristics and temporal features of glomerular activity thus should be investigated in a future study. In addition, there can be an overfitting problem because all of the odorant sets are composed of a small number of odorants. Misclassification could occur if data near the boundary between the similar and dissimilar classes were eliminated when performing leave-one-out validation. However, it is difficult to increase the size of the odorant because it is difficult to find a pair of single component odors that smell similar. This problem will be solved if glomerular activity patterns of odorant mixture become predictable, which we plan to accomplish in a future study.

Conclusions

In this article, human perception was compared with indices extracted from activity patterns evoked in the glomerular layer of the olfactory bulb in rats. The correlation achieved with the proposed method was equal to or higher than that of physicochemical descriptors. Similarities between odorants were also predicted using a neural network of 3 indices used to define the similarity between activity patterns. The results showed a prediction accuracy of 64–92%, supporting the potential for prediction of olfactory perception using activity patterns. Combining this approach with the authors' previously proposed method of predicting glomerular activity from odorant molecular structures (Soh *et al.* 2011) may provide a technique for predicting human perception based on such structures.

Although the proposed method showed a certain correlation with human perception, the indices were empirically defined rather than being based on information processing mechanisms in olfactory systems. It should be noted that dynamic information processing in the olfactory system is likely to have a considerable impact on perception. A number of olfactory models involving different neurodynamic architectures have been presented in previous studies, and these can be used for further development of the proposed method. For example, Cleland and Sethupathy (2006) proposed a model that considers contrast enhancement in the olfactory bulb, and Li (1990) described a model that simulates cross-adaptation between odors. These models can provide highly suitable indices for the prediction of perceptual characteristics. In future studies, we intend to define more efficient and accurate features for predicting human olfactory perceptions and to create a sensory model that can be used to assess such perceptions.

Funding

This work was supported by a Grant-in-Aid for Japan Society for Promotion of Science Fellows [11J10869].

Acknowledgments

The authors express their gratitude to Prof. Dr Michel Leon at University of California, Irvine, for providing valuable advice about usage of glomerular activity data and for the database "Glomerular Activity Response Archive." The authors are grateful to Prof. Dr Kouich Hashimoto for continuing interest and encouragement.

References

Branca A, Simonian P, Ferrante M, Novas E, Negri RM. 2003. Electronic nose based discrimination of a perfumery compound in a fragrance. Sensors and Actuators B: Chemical. 92(1–2):222–227.

Buck L, Axel R. 1991. A novel multigene family may encode odorant receptors: a molecular basis for odor recognition. Cell. 65(1):175–187.

Cleland TA, Johnson BA, Leon M, Linster C. 2007. Relational representation in the olfactory system. Proc Natl Acad Sci USA. 104(6):1953–1958.

Cleland TA, Sethupathy P. 2006. Non-topographical contrast enhancement in the olfactory bulb. BMC Neurosci. 7:7.

Bernt S, Crowley JL. 2000. Recognition without correspondence using multidimensional receptive field histograms. Int J Comput Vision. 36:31–50.

Ehret B, Safenreiter K, Lorenz F, Biermann J. 2011. A new feature extraction method for odour classification. Sens Actuat B Chem. 158(1):75–88.

Falasconi M, Gutierrez-Galvez A, Leon M, Johnson BA, Marco S. 2012. Cluster analysis of rat olfactory bulb responses to diverse odorants. Chem Senses. 37:639–653.

Farahbod H, Johnson B, Minami SS, Leon M. 2006. Chemotopic representations of aromatic odorants in the rat olfactory bulb. J Comparat Neurol. 366:350–366.

Firestein S. 2001. How the olfactory system makes sense of scents. Nature. 413(6852):211–218.

Haddad R, Khan R, Takahashi YK, Mori K, Harel D, Sobel N. 2008. A metric for odorant comparison. Nat Methods. 5(5):425–429.

Haddad R, Lapid H, Harel D, Sobel N. 2008. Measuring smells. Curr Opin Neurobiol. 18(4):438–444.

Haddad R, Medhanie A, Roth Y, Harel D, Sobel N. 2010. Predicting odor pleasantness with an electronic nose. PLoS Comput Biol. 6(4):e1000740.

Johnson BA, Arguello S, Leon M. 2007. Odorants with multiple oxygen-containing functional groups and other odorants with high water solubility preferentially activate posterior olfactory bulb glomeruli. J Comp Neurol. 502(3):468–482.

Johnson BA, Farahbod H, Leon M. 2005. Interactions between odorant functional group and hydrocarbon structure influence activity in glomerular response modules in the rat olfactory bulb. J Comp Neurol. 483(2):205–216.

Johnson BA, Farahbod H, Xu Z, Saber S, Leon M. 2004. Local and global chemotopic organization: general features of the glomerular representations of aliphatic odorants differing in carbon number. J Comp Neurol. 480(2):234–249.

Johnson BA, Woo CC, Leon M. 1998. Spatial coding of odorant features in the glomerular layer of the rat olfactory bulb. J Comp Neurol. 393(4):457–471.

Johnson BZ, Ho SL, Xu Z, Yihan JS, Yip S, Hingco EE, Leon M. 2002. Functional mapping of the rat olfactory bulb using diverse odorants reveals modular responses to functional groups and hydrocarbon structural features. J Comp Neurol. 449(2):180–194.

Kaeppler K, Mueller F. 2013. Odor classification: a review of factors influencing perception-based odor arrangements. Chem Senses. 38(3):189–209.

Khan RM, Luk CH, Flinker A, Aggarwal A, Lapid H, Haddad R, Sobel N. 2007. Predicting odor pleasantness from odorant structure: pleasantness as a reflection of the physical world. J Neurosci. 27(37):10015–10023.

Le Berre E, Atanasova B, Langlois D, Etiévant P, Thomas-Danguin T. 2007. Impact of ethanol on the perception of wine odorant mixtures. Food Quality and Preference. 18(6):901–908.

Li Z. 1990. A model of olfactory adaptation and sensitivity enhancement in the olfactory bulb. Biol Cybern. 62(4):349–361.

Mandairon N, Poncelet J, Bensafi M, Didier A. 2009. Humans and mice express similar olfactory preferences. PLoS One. 4(1):e4209.

Mori K, Nagao H, Yoshihara Y. 1999. The olfactory bulb: coding and processing of odor molecule information. Science. 286(5440):711–715.

Mori K, Sakano H. 2011. How is the olfactory map formed and interpreted in the mammalian brain? Annu Rev Neurosci. 34:467–499.

Perrin L, Symoneaux R, Maître I, Asselin C, Jourjon F, Pagès J. 2008. Comparison of three sensory methods for use with the Napping® procedure: Case of ten wines from Loire valley. Food Quality Prefer. 19(1):1–11.

Persaud K, Dodd G. 1982. Analysis of discrimination mechanisms in the mammalian olfactory system using a model nose. Nature. 299(5881):352–355.

Saito H, Chi Q, Zhuang H, Matsunami H, Mainland JD. 2009. Odor coding by a Mammalian receptor repertoire. Sci Signal. 2(60):ra9.

Sato S. 1978. Introduction to sensory test (in Japanese.) Tokyo (Japan): JUSE Press Ltd. p. 7–13.

Soh Z, Tsuji T, Takiguchi N, Ohtake H. 2011. An artificial neural network approach for glomerular activity pattern prediction using the graph kernel method and the Gaussian mixture functions. Chem Senses. 36(5):413–424.

Talete srl. 2011. DRAGON (Software for Molecular Descriptor Calculation) Version 6.0, 2011. Available from: http://www.talete.mi.it/

Tsuji T, Fukuda O, Ichinobe H, Kaneko M. 1999. A log-linearized Gaussian mixture network and its application to EEG pattern classification. IEEE Transact Syst Man Cybernet C Appl Rev. 29:60–72.

Uchida N, Takahashi YK, Tanifuji M, Mori K. 2000. Odor maps in the mammalian olfactory bulb: domain organization and odorant structural features. Nat Neurosci. 3(10):1035–1043.

Utsunomiya H, Isogai A, Iwata H, Nakano S. 2006. Flavor terminology and reference standards for sensory analysis of sake (in Japanese.) J Brew Soc Japan. 101:730–739.

Xu F, Liu N, Kida I, Rothman DL, Hyder F, Shepherd GM. 2003. Odor maps of aldehydes and esters revealed by functional MRI in the glomerular layer of the mouse olfactory bulb. Proc Natl Acad Sci USA. 100(19):11029–11034.

Youngentob SL, Johnson BA, Leon M, Sheehe PR, Kent PF. 2006. Predicting odorant quality perceptions from multidimensional scaling of olfactory bulb glomerular activity patterns. Behav Neurosci. 120(6):1337–1345.

Zhang X, Firestein S. 2002. The olfactory receptor gene superfamily of the mouse. Nat Neurosci. 5(2):124–133.